JOURNAL OF NATURAL PRODUCTS

ARTICLE

pubs.acs.org/jnp

Phomalevones A−C: Dimeric and Pseudodimeric Polyketides from a Fungicolous Hawaiian Isolate of *Phoma* sp. (Cucurbitariaceae)

Sang Hee Shim,[†,‡] Jonas Baltrusaitis,[†] James B. Gloer,[*,†] and Donald T. Wicklow[§]

[†]Department of Chemistry, University of Iowa, Iowa City, Iowa 52242, United States

[‡]School of Biotechnology, Yeungnam University, Gyeongsan 712-749 Korea

[§]Bacterial Foodborne Pathogens and Mycology Research Unit, Agricultural Research Service, National Center for Agricultural Utilization Research, USDA, Peoria, Illinois 61604, United States

Supporting Information

ABSTRACT: Phomalevones A−C (**1**−**3**), three new compounds with bis-dihydroxanthone and bis-benzophenone systems, were isolated from cultures of a Hawaiian isolate of *Phoma* sp. (MYC-1734 = NRRL 39060; Cucurbitariaceae). The structures of **1**−**3** were determined by analysis of NMR and MS data. The absolute configurations of the sp^3 stereocenters in the monomeric unit of **1** were assigned by application of Mosher's method, and overall absolute configurations were proposed on the basis of ECD data using both computational methods and comparisons with literature data for model compounds. All three compounds showed antibacterial activity, and compounds **2** and **3** also exhibited antifungal effects.

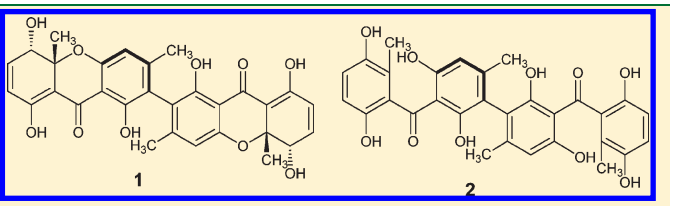

Our chemical studies of mycoparasitic and fungicolous fungi have led to the isolation of a variety of novel metabolites with antifungal effects and other biological activities.[1−5] In the course of our ongoing studies of these types of fungi, an undescribed fungicolous isolate of *Phoma* sp. (MYC-1734 = NRRL 39060; Cucurbitariaceae) collected in Hawaii was subjected to chemical investigation. This isolate was initially identified as *Phoma leveillei* var. *microspora* Gruyter & Boerema on the basis of its morphological characteristics. However, detailed DNA sequence information and subsequent database queries suggested that this isolate may represent a new species, and it is therefore referred to here only as *Phoma* sp. An EtOAc extract from cultures of this isolate showed potent antifungal activity in preliminary assays. Chemical investigation of this extract led to the discovery of a new symmetrical dihydroxanthone dimer that we named phomalevone A (**1**), a symmetrical benzophenone dimer (phomalevone B; **2**), and a related pseudodimeric metabolite (phomalevone C; **3**). The isolation, structure determination, and biological activities of **1**−**3** are described here.

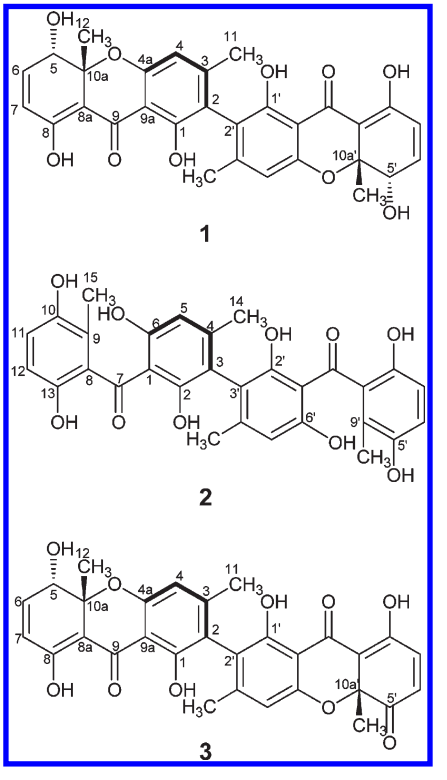

RESULTS AND DISCUSSION

Fractionation of the crude EtOAc extract of solid-substrate fermentation cultures of MYC-1734 by Sephadex LH-20 column chromatography afforded phomalevones A−C (**1**−**3**) as the major components. The molecular formula of phomalevone A (**1**) was determined to be $C_{30}H_{26}O_{10}$ (18 unsaturations) by HRESIMS. The presence of only 15 signals in the ^{13}C NMR spectrum indicated a symmetrical, homodimeric structure. Analysis of ^{1}H and ^{13}C NMR and DEPT spectra (Table 1) revealed that each half of the molecule possessed one cross-conjugated ketone group, one aryl methyl, one methyl group attached to a quaternary sp^3 carbon,

Special Issue: Special Issue in Honor of Koji Nakanishi

Received: November 1, 2010
Published: January 19, 2011

dx.doi.org/10.1021/np100791b | *J. Nat. Prod.* 2011, 74, 395–401

Table 1. NMR Data for Phomalevone A (1)[a]

position	δ_H[a] (mult.; J in Hz)	δ_C	HMBC (H# → C#)
1/1′	11.75 s; OH	159.6	1, 2, 3, 9, 9a
2/2′		116.9	
3/3′		150.0	
4/4′	6.42 s	109.8	2, 11, 4a, 9a, 9[b]
4a/4a′		157.0	
5/5′	4.21 d (6.0)	68.6	6, 7, 8a, 9, 10a, 12
6/6′	6.61 dd (6.0, 10)	137.9	5, 8, 10a
7/7′	6.22 d (10)	126.7	5, 6, 8a, 9[b]
8/8′	13.58 s, OH	166.4	7, 8, 8a
8a/8a′		103.6	
9/9′		186.8	
9a/9a′		104.9	
10a/10a′		80.2	
11/11′	2.07 s	21.1	2, 3, 4
12/12′	1.51 s	24.0	5, 8a, 10a

[a] Data were recorded for a $CDCl_3$ solution at 400 MHz (^1H), 100 MHz (^{13}C), and 600 MHz (HMBC). [b] Four-bond correlations.

seven nonprotonated sp^2 carbons, three sp^2 methine units (two of which were vicinally coupled), and one sp^3 oxymethine unit. Two hydrogen-bonded phenolic proton signals (δ_H 13.58 and 11.75) were observed. One additional OH group was presumed to be present on the basis of the DEPT data. Accordingly, a tricyclic substructure was required for each half of **1** to fulfill the unsaturation requirement.

An isolated O−CH−CH═CH spin-system corresponding to the C5−C7 unit in **1** was assigned on the basis of $^1H-^1H$ COSY data and coupling data for the corresponding signals. Each tricyclic unit was constructed on the basis of HMBC correlations and NMR chemical shifts. HMBC correlations of H_3-12 (the methyl group attached to a quaternary sp^3 carbon) with C-5, C-10a, and C-8a and of the 8-O*H* proton with C-7, C-8, and C-8a allowed connection of the C5−C7 unit to C-8 and C-10a to construct a partially reduced benzene ring. In addition, HMBC correlations of the aryl methyl signal with C-2, C-3, and C-4 and of the 1-O*H* with C-1, C-2, and C-9a enabled assignment of the C9a−C4 unit. This unit was connected with C-4a to complete the benzene ring based on HMBC correlations of H-4 with C-2, C-11, C-4a, and C-9a.

At this point, a ketocarbonyl unit, another oxygen atom, and one ring remained to be assigned. Linkage of the two rings at C-8a and C-9a via the carbonyl carbon was established by four-bond HMBC correlations of 1-O*H*, H-4, H-5, and H-7 with the carbonyl carbon (C-9). In addition, the molecular formula and the downfield chemical shifts of C-10a and C-4a indicated the presence of an ether linkage between these two positions, thereby forming a third ring and completing a xanthone-type system. Thus, the structure of each monomeric half of **1** was established as shown. The strong correlation from the hydrogen-bonded phenolic proton (1-O*H*; δ_H 11.75) to the nonprotonated aromatic carbon C-2 (δ_C 116.9) indicated that the two units are joined via a C-2−C-2′ linkage, rather than a C-4−C-4′ linkage, which some fungal xanthone dimers are known to possess.[6−8]

A strong NOESY correlation between H_3-12 and H-5 indicated that they are on the same face of the molecule, as the C8a−C10a ring fusion is likely to favor a conformation that places the CH_3 group in a pseudoaxial orientation (ChemBio3D 11.0.1). The presence of a secondary alcohol moiety in **1** suggested that it might be suitable for stereochemical analysis using Mosher's method.[9,10]

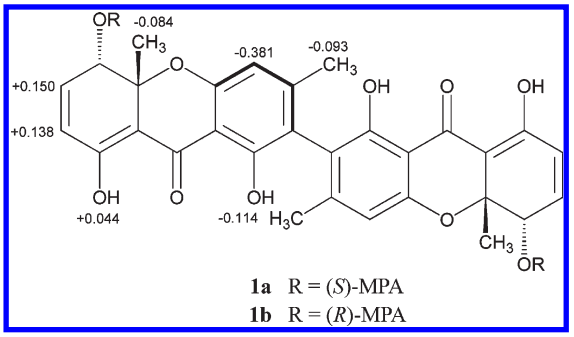

Figure 1. Observed chemical shift differences ($\Delta\delta = \delta_S - \delta_R$, ppm, 400 MHz) for the (*R*)- and (*S*)-MPA esters of phomalevone A (**1**).

Treatment of **1** with (*S*)-MPAOH (α-methoxyphenylacetic acid) or (*R*)-MPAOH in the presence of 1-ethyl-3-(3-dimethylaminopropyl)carbodiimide and DMAP afforded the (*S*)-MPA ester (**1a**) or (*R*)-MPA ester (**1b**), respectively. Formation of the esters was confirmed in each case by a significant downfield shift of the signal for H-5 and the appearance of the expected new aromatic and methoxy signals in the ^1H NMR spectrum. ^1H NMR signals for **1a** and **1b** were assigned by comparison with the data for **1**. Upon comparison of ^1H NMR chemical shifts for **1a** and **1b** ($\Delta\delta$ values shown in Figure 1), the $\Delta\delta$ values observed for major signals of **1a** and **1b** (Figure 1) were consistent with assignment of the *S*-configuration at C-5, leading to the proposal of *S*- and *R*-absolute configurations at C-5/5′ and C10a/10a′, respectively.

The ECD (electronic circular dichroism) spectra of secalonic acids (dimeric fungal tetrahydroxanthone derivatives) show a large Cotton effect at 330−335 nm, which has been correlated with the stereochemical environment at C-10a (C-10a′).[8,11,12] Secalonic acids A and G, which possess an *S*-configuration at C-10a (C-10a′), are reported to show a negative Cotton effect, whereas secalonic acids D and F, with an *R*-configuration at C-10a (C-10a′), displayed a positive Cotton effect.[11−14] According to these precedents, phomalevone A (**1**) would seem likely to display a positive Cotton effect at approximately 330 nm in its ECD spectrum, assuming an analogous *S*-configuration at C-10a. Positive Cotton effects (CEs) are indeed observed at 300 and 375 nm. However, it is risky to compare these data directly because **1** has a CH_3 group at this position, rather than a $COOCH_3$ group. Moreover, the situation in this case is complicated by the presence of a considerable barrier to rotation at the C2−C-2′ bond, which results in the presence of a preferred atropisomer (rotational isomer), and this seems to have considerable influence on the ECD data obtained (see below).

Phomalevone B (**2**) was determined to be an isomer of **1** on the basis of HRESIMS data. Its ^{13}C NMR spectrum again showed 15 carbon signals, indicating that **2** also has a symmetrical, homodimeric structure. The NMR spectra for **2** were recorded in methanol-d_4 due to its poor solubility in $CDCl_3$ and substantial signal overlap that was observed when the ^1H NMR spectrum was recorded in acetone-d_6. Although no exchangeable proton signals were observed in the ^1H NMR spectrum recorded in methanol-d_4, the presence of eight OH groups could be assumed on the basis of ^{13}C and DEPT NMR data, together with the molecular formula. Signals for two *ortho*-coupled, upfield-shifted aromatic protons (δ 6.63, d, J = 8.4 Hz and 6.58, d, J = 8.4 Hz), one isolated aromatic proton (δ 6.35, s), and two aryl methyls (δ 1.98, s and 2.03, s) were observed in the ^1H NMR spectrum, suggesting some analogy to **1**. However, a significant downfield shift of the only carbonyl signal relative to its location in the spectrum of **1** (from δ_C 186.8 in **1** to

dx.doi.org/10.1021/np100791b | J. Nat. Prod. 2011, 74, 395–401

δ_C 203.9 in **2**) and the presence of two additional sp^2 carbon signals in place of the C-5 and C-10a sp^3 signals in the spectrum of **1** suggested that **2** has a benzophenone system rather than a dihydroxanthone structure. Similar relationships have been previously observed among other co-occurring fungal metabolites.[14] HMBC correlations of H_3-14 with C-3, C-4, and C-5 and of H_3-15 with C-8, C-9, and C-10 indicated that the two aryl methyl groups are attached to C-4 and C-9, respectively, and identified the two carbons flanking each methyl group.

The positions of the four hydroxy groups in each monomer unit were assigned on the basis of ^{13}C NMR chemical shifts, along with HMBC correlations of aromatic protons with nearby carbons. Comparison of the spectroscopic data with those of phomalevone A (**1**) and acremonidin D, another symmetrical dimer with two benzophenone monomer units connected via a methylene linkage,[15] were also useful in supporting the structural assignment. HMBC correlations of vicinal aromatic protons H-11 and H-12 with oxygenated carbons C-10 and C-13 completed the construction of the C8−C13 benzene ring. Chemical shift values for the second benzene ring were consistent with a 1,3-dioxygenated pattern. HMBC correlations of the isolated aryl proton H-5 with C-1, C-3, C-6, C-14, and C-7, together with those noted above for H_3-14, led to assignment of structure **2** as shown. This connectivity is consistent with the close spectroscopic analogy to **1**. Analysis of optical rotation and ECD data for **2** indicates that it is present as a preferred atropisomer. This issue is addressed further below.

Phomalevone C (**3**) was determined to have the formula $C_{30}H_{24}O_{10}$ (19 unsaturations) by HRESIMS. Unlike symmetrical dimers **1** and **2**, the NMR data for **3** indicated an unsymmetrical, pseudodimeric structure. In fact, two sets of very closely paired ^1H and ^{13}C NMR signals were observed in the corresponding individual spectra (including nearly 60 discrete ^{13}C NMR signals, rather than the 30 signals that would be expected for an unsymmetrical pseudodimeric structure). These data suggested that the sample contained a mixture of two closely related pseudodimeric compounds in a 1:1 ratio, but all efforts to resolve components of the sample by HPLC were unsuccessful. Analysis of 1D and 2D NMR spectra, particularly HMBC data, revealed that **3** is a heterodimer in which one subunit is the same as the monomer unit in **1**, while the other is the same except that the secondary alcohol group is oxidized to a carbonyl group. Correlations and shifts for half of the signals matched very closely with those observed for **1**. Values observed for the other half were nearly identical except for HMBC correlations of H_3-12′ and H-7′ with a second ketocarbonyl carbon (δ_C 196.0 and 196.2), rather than a secondary alcohol carbon as in **1**. The C-2−C-2′ connection between the two units of **3** was confirmed by HMBC correlations of the 1-O*H* signal (δ_H 11.82 and 11.75) with a nonprotonated aromatic carbon (C-2; δ_C 116.46 and 116.51) and of the 1′-O*H* signal (δ_H 11.51) with the analogous carbon C-2′ (δ_C 117.25 and 117.20). As was the case for **1**, a strong NOESY correlation of H-5 and H_3-12 indicated that the C-5 hydroxy group and CH_3-12 are *trans* to each other in **3**. The absolute configurations at the sp^3 stereocenters in **3** are assumed to be analogous to those of **1**.

It was presumed that observation of two sets of NMR signals for **3** was associated with the fact that there is a significant barrier to rotation at the biaryl linkage in these compounds. However, our inability to separate the two species evident in the spectrum of **3** by HPLC led to consideration of other possible explanations, such as whether **3** could exist as a mixture of tautomers that would not be observed for reduced analogue **1**. Variable-temperature NMR experiments using DMSO-d_6 as solvent failed to provide useful information about either possibility because **3** slowly decomposed in DMSO-d_6, even at room temperature. No signal coalescence was observed at temperatures up to 60 °C when data were collected using $CDCl_3$, methanol-d_4, or acetone-d_6, or down to −60 °C using methanol-d_4. Addition of Na_2CO_3 to solutions of **3** in $CDCl_3$ or methanol-d_4 did not result in any differences in the ^1H NMR spectra. Thus, further analysis focused on the rotational isomerism issue.

According to prior studies of biphenyl and other biaryl derivatives having hydroxy and methyl substituents in positions *ortho* to the connection point (e.g., gossypol),[16] the corresponding rotamers do not readily interconvert due to an energy barrier that is over 50 kcal/mol. Analysis of compound **2**, which lacks sp^3-hybridized stereocenters, revealed a specific rotation of +82, which is consistent with the presence of such a barrier and with the prevalence of one of the two possible atropisomers of **2**. Moreover, the ECD spectrum of **2** bears very close resemblance to that of **1** (Figure 2), strongly suggesting that **1** and **2** are present in analogous rotameric forms. Because the shapes of the curves below 310 nm are so similar (Figure 2), and because the only stereochemical feature of **2** is the rotational one, it appears that the shape of the ECD spectrum below 310 is diagnostic for the rotational form present. If both rotamers of **1** were present, and simply inseparable, they should be diastereomeric due to the existing sp^3 stereocenters elsewhere in the molecule, but the NMR data indicated the presence of only one species, while the ECD data suggested only one rotameric form, as noted above. Despite the observation of a 1:1 ratio of two sets of NMR signals for the sample of **3**, the ECD spectrum of **3** (Figure 2) clearly had the same basic shape as **1** and **2** in the relevant region, indicating the presence of the same rotameric form (i.e., indicating that **1**−**3** all have the same axial stereochemical configuration at the dimeric or pseudodimeric linkage). The presence of two diastereomeric forms of **3** in a 1:1 ratio, with both diastereomers retaining the a*S* chirality could be due to formation of **3** via differential modification at either end of a suitable atropisomer (e.g., of **1** or **2**) or to a lack of stereoselectivity in the process of forming relevant sp^3 stereocenters, although the latter seems less likely. The resulting compounds would be diastereomeric, so that each would be expected to show a slightly different set of 30 NMR signals and might well be exceptionally difficult to separate.

Assuming that **1**−**3** all have the same axial/rotameric configuration, the remaining question is whether these systems display a*R* (= *M*) or a*S* (= *P*) chirality. There does not appear to be an empirical rule that would unambiguously apply to this case, but literature data for simpler model compounds were useful in suggesting a possible assignment. Bringmann et al.[17] showed that a series of compounds containing only the biphenyl core unit with substituents otherwise similar to those of **2** afforded CD spectra with some consistent features. The a*S* (= *P*) isomers of the closest analogues showed CD curves that bear resemblance to those of **1**−**3**, with the a*R* (= *M*) isomers showing an inverse relationship.[17] For example, the a*R* isomer of a biphenyl derivative analogous to **2** except for the presence of CH_3CO groups in place of the outer benzoyl units of **2** and methoxy groups in place of the 1/1′ hydroxy groups showed a strong positive CE at 211 nm, weaker negative CEs at 241 and 310 nm, and a weaker positive CE at 267 nm,[17] whereas **2** shows a strong negative CE at 216 nm, weaker positive CEs at 242 and 300 nm, and a weaker negative CE at 275 (Figure 2). The sequential positive and negative CEs near 240 and 201 nm, respectively, in the CD spectra of **1**−**3** suggest *P*-helicity and assignment of the a*S*-configuration for all three

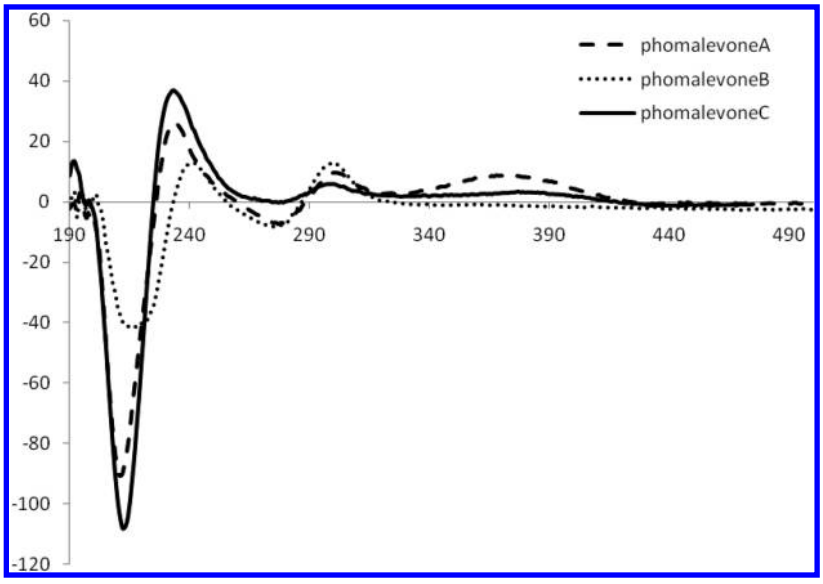

Figure 2. Experimental ECD spectra of phomalevones A−C (**1**−**3**).

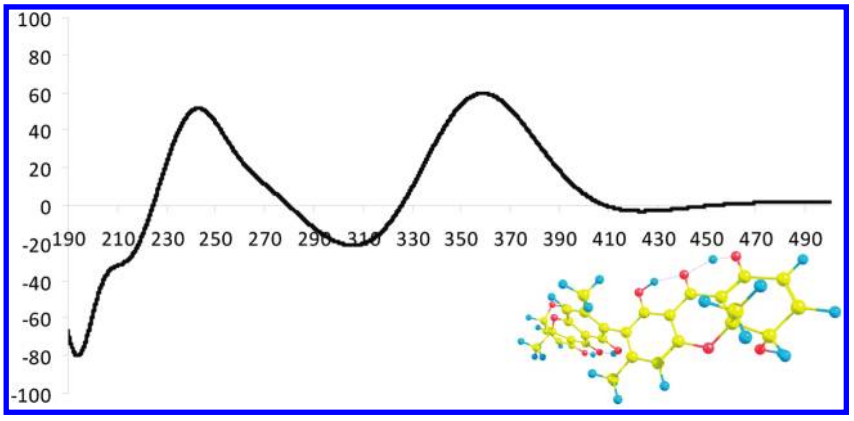

Figure 3. Calculated ECD spectrum and energy-minimized model of a*S*-phomalevone A (**1**).

compounds. The corresponding exciton chirality is supported by the occurrence of UV absorptions appearing roughly halfway between these low-wavelength positive and negative CEs.

Ultimately, because of the more elaborate structures being analyzed in this case, independent support for assignment of an a*S*-configuration to **1**−**3** was sought through computational methods. Given the added complexity associated with structure **3**, attention was focused on **1** and **2**. After geometry optimization of each structure to obtain the two minimum energy conformers (corresponding to the two possible rotameric forms), TDDFT-calculated, smoothed ECD spectra were generated for each rotamer and compared with the experimental ECD spectra (Figure 2). In the case of **1**, significant resemblance between the experimental and calculated spectra for the a*S* atropisomer was evident (Figure 3). Although the relative intensities and precise locations of the individual peaks differ, each spectrum shows a negative CE below 225 nm, a positive CE near 240 nm, a weak negative CE centered at a somewhat more different position (280 vs 308), and positive CE(s) beyond.

In the case of **2**, the calculated ECD data initially obtained resembled neither the experimental spectrum nor its inverse. However, inspection of the energy-minimized conformer of **2** (and its enantiomeric rotamer) revealed that the added flexibility associated with the presence of benzophenone units rather than dihydroxanthone units had led to significant differences in overall shape compared to **1**. This difference was due mainly to H-bonding of the ketone carbonyl oxygen in **2** with OH-6/6′, rather than with OH-2/2′: the latter would give an overall shape more like that of the relatively rigid structure **2**. Upon adjustment of the structure to reflect H-bonding between the carbonyl and OH-2/2′, followed by reoptimization, it was found that the resulting conformer having the a*S*-configuration afforded a calculated ECD spectrum that somewhat more closely resembled the calculated spectrum for **1** and the experimental data for **1** and **2** (Figure 4). Upon further analysis, it was found that, while both conformers have similar energies, the conformer of **2** displaying H-bonding between the carbonyl group and H-2/2′ (as shown in Figure 4) is lower in energy in simulated methanol solution (using the COSMO solvation model), while the conformer displaying H-bonding between the carbonyl and H-6/6′ has lower energy in the gas phase. Comparison of the calculated and experimental ECD data for **2** showed a bit less resemblance than in the case of **1**, but in each spectrum, a low λ, weak negative CE is followed by a positive CE near 240 nm and an additional positive CE near 300 nm. On the basis of these results, comparison with model compounds as noted above, and the close similarity in

dx.doi.org/10.1021/np100791b |*J. Nat. Prod.* 2011, 74, 395–401

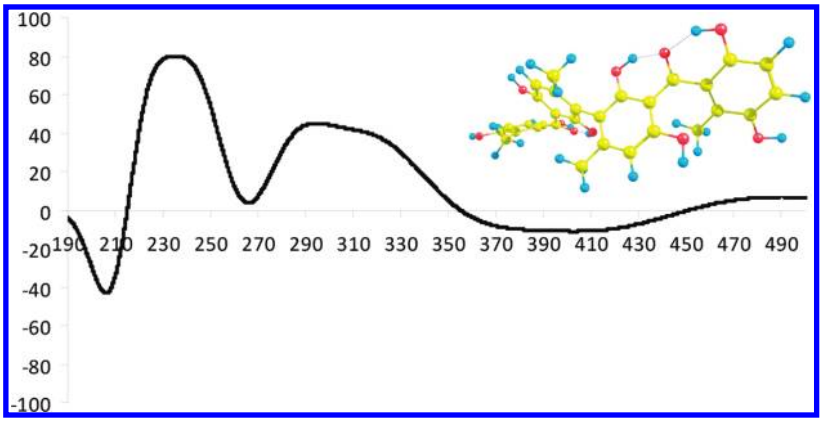

Figure 4. Calculated ECD spectrum and energy-minimized model of a*S*-phomalevone B (**2**).

their ECD spectra, compounds **1**−**3** are all proposed to have the a*S* axial configuration.

Many dihydroxanthone and tetrahydroxanthone derivatives have been reported from fungi such as *Emericella*, *Gelatinospora*, *Penicillium*, *Phomopsis*, and *Aspergillus*.[6−8] Dimeric and pseudodimeric analogues are less common, but have been reported.[6,18−23] The closest analogues to **1**−**3** have been reported as bioactive metabolites of a *Ceuthospora* sp.[18] and *Aschersonia luteola*,[19] with the latter (ascherxanthone B) showing antifungal activity against the rice blast fungal pathogen *Magnaporthe grisea*. The occurrence of **1** together with benzophenone-containing analogue **2** is consistent with literature precedents indicating that hydroxylated benzophenones are key intermediates in xanthone biosynthesis.[24−26]

Phomalevone A (**1**) showed antibacterial activity in standard agar disk diffusion assays[27,28] at 100 μg/disk against *Bacillus subtilis* (ATCC 6051) and *Staphylococcus aureus* (ATCC 29213), causing inhibitory zones of 36 and 23 mm, respectively. Phomalevone B (**2**) was also active against *B. subtilis*, *S. aureus*, *Candida albicans* (ATCC 14053), and *Escherichia coli* (ATCC 25922) at the same level, affording zones of 38, 26, 18, and 18 mm, respectively. Phomalevone C (**3**) showed potent activity against *B. subtilis* and *S. aureus* at this level, causing inhibitory zones of 34 and 22 mm, respectively. A gentamicin sulfate standard gave 20- to 25-mm clear zones in these antibacterial assays at 25 μg/disk. Phomalevone C (**3**) also exhibited activity in disk assays against *Aspergillus flavus* (NRRL 6541) and *Fusarium verticillioides* (NRRL 25457), causing inhibition zones of 10 mm in each case at 200 μg/disk, and showed an MIC value[29] against *F. verticillioides* of approximately 10 μg/mL. Compound **3** did not show complete inhibition of *A. flavus* at concentrations up to 25 μg/mL, but did afford an IC_{50} value of 4 μg/mL. Nystatin, an antifungal standard, afforded MIC values of approximately 10 μg/mL in both assays and IC_{50} values of 5 and 3 μg/mL, respectively, using the same protocols.

EXPERIMENTAL SECTION

General Experimental Procedures. Optical rotations were measured on a JASCO model DIP-1000 digital polarimeter. UV data were recorded with a Varian Cary III UV−visible spectrometer, and ECD data were collected using an Olis Cary-17 spectrophotometer (0.1-cm cell). NMR spectra were recorded in $CDCl_3$ or methanol-d_4, and chemical shifts were referenced relative to the corresponding signals (δ_H 7.24/δ_C 77.23 for $CDCl_3$; δ_H 3.31/δ_C 49.15 for methanol-d_4). ^{1}H NMR data were recorded at 400 MHz (Bruker DRX-400) or 600 MHz (Bruker AMX-600). ^{13}C NMR data were recorded at 100 MHz (DRX-400). All 2D NMR data were recorded at 600 MHz (^{1}H dimension). HRESIMS data were recorded using a Fisons Autospec double-focusing mass spectrometer. All HPLC separations were carried out using an Alltech HS Hyperprep 100 BDS phenyl semipreparative column (10 × 250 mm) at a flow rate of 2 mL/min. Other general procedures and instrumentation have been described previously.[29,30]

Fungal Material. The culture employed in this work (MYC-1734) was originally isolated by D.T.W. from a white mycelial growth on the undersurface of a dead hardwood branch that was collected in a montane dry forest (Ohi'a), Koloko Hue Street, Kailua-Kona, Hawaii Co., HI, by D.T.W. in November 2002. A subculture has been deposited at the Agricultural Research Service (ARS) Culture Collection with the accession number NRRL 39060. This isolate was initially identified as *Phoma leveillei* var. *microspora* Gruyter & Boerema based on *in vitro* colony growth, conidiogenesis, and micromorphology.[31] However, on the basis of DNA sequence analyses, de Gruyter et al. recently introduced the genus *Pyrenochaetopsis* (Cucurbitariaceae) to accommodate certain species of *Pyrenochaeta* and *Phoma*, including *P. leveillei* var. *microspora*.[32] The culture was subjected to partial sequence analysis of the internal transcribed spacer region (ITS) and domains D1 and D2 of the nuclear large subunit (28S) rDNA gene using ITS5 and NL4 as polymerase chain reaction and sequencing primers.[33,34] A nucleotide-to-nucleotide BLAST query of the GenBank database (http://www.ncbi.nlm.nih.gov/BLAST) recovered #GQ153264 "Dothideomycetes sp." as the closest match to the ITS DNA of NRRL 39060 (93%). A similar blast query, using the partial 28S rDNA of NRRL 39060, yielded *Camarosporium* sp. (Cucubitariaceae) as the closest match (97%) while yielding strains of *Pyrenochaetopsis microspora* and *P. leptospora* at equivalent identities (95%). These results suggest that NRRL 39060 may represent a new species. Because of the uncertainties associated with these percentages of nucleotide sequence divergence, we conservatively characterize this isolate at present only as "*Phoma* sp." The sequence was deposited in GenBank (National Center for Biotechnology Information) as HM751085. General fermentation and extraction procedures employed have been described elsewhere.[30]

Isolation. The crude extract (2.3 g) obtained from eight 500-mL fermentation flasks each containing 50 g of rice was first partitioned between hexanes (3 × 100 mL) and CH_3CN (50 mL), and the CH_3CN-soluble portion (1.4 g) was fractioned by Sephadex LH-20 column chromatography using a hexanes−$CHCl_3$ solvent gradient. A 50-mg portion of the fraction eluted with 80:20 hexanes−$CHCl_3$ (801 mg) was further separated by reversed-phase HPLC (30 to 100% CH_3CN in H_2O over 40 min) to afford five fractions. The second subfraction (20 mg) was further separated by reversed-phase HPLC (30% CH_3CN in H_2O over 50 min) to afford phomalevone A (**1**; 9 mg). The fifth subfraction (20 mg) was repeatedly separated by reversed-phase HPLC (30% CH_3CN in H_2O over 50 min) to afford phomalevone B (**2**; 5 mg). A 30-mg portion of the fraction eluted with 60:40 hexanes−$CHCl_3$ (105 mg) was separated by

semipreparative reversed-phase HPLC (50% CH_3CN in H_2O over 45 min) to provide phomalevone C (**3**; 9.0 mg).

*Phomalevone A (**1**):* yellow solid; $[\alpha]_D$ +193 (c 1.33 × 10^{-3} g/mL, $CHCl_3$, 25 °C); UV λ_{max} (MeOH; log ε) 206 (4.60), 230 (sh, 4.43), 288 (4.17), 383 nm (4.36); ECD (MeOH; $\Delta\varepsilon$) 213 (−90), 236 (+25), 278 (−6), 302 (+9), 373 (+8); ^{1}H NMR, ^{13}C NMR, and HMBC data, see Table 1; NOESY correlations ($CDCl_3$, H-# → H-#) H-4 ↔ H_3-11; H-5 ↔ H-6 and H_3-12; H-6 ↔ H-5 and H-7; HRESIMS obsd m/z 547.1590 $[M + H]^+$, calcd for $C_{30}H_{27}O_{10}$, 547.1604.

*Phomalevone B (**2**):* yellow solid; $[\alpha]_D$ +82 (c 0.53 × 10^{-3} g/mL, MeOH, 25 °C); UV λ_{max} MeOH (log ε) 215 (4.81), 292 (4.59), 362 nm (4.01); ECD (MeOH; $\Delta\varepsilon$) 216 (−41), 242 (+12), 275 (−8), 300 (+12); ^{1}H NMR (400 MHz, methanol-d_4) δ 6.63 (d, J = 8.4 Hz, H-11 and H-11′), 6.58 (d, J = 8.4 Hz, H-12 and H-12′), 6.35 (s, H-5 and H-5′), 2.03 (s, H_3-15 and H_3-15′), 1.98 (s, H_3-14 and H_3-14′); ^{13}C NMR (100 MHz, methanol-d_4) δ 203.9 (C-7/C-7′), 162.6 (C-6 and C-6′), 162.4 (C-2/C-2′), 150.7 (C-4/C-4′), 149.5 (C-10/C-10′), 147.0 (C-13/C-13′), 134.2 (C-8/C-8′), 122.3 (C-9/C-9′), 116.5 (C-11/C-11′), 115.8 (C-3/C-3′), 114.5 (C-12/C-12′), 111.1 (C-1/C-1′), 109.6 (C-5/C-5′), 20.9 (C-14/C-14′), 12.9 (C-15/C-15′); HMBC correlations (methanol-d_4, H-# → C-#) H-5 → C-1, C-3, C-6, C-14, and C-7; H-11 → C-9, C-10, C-12, C-13, C-8, and C-15; H-12 → C-8, C-10, C-11, C-13, C-7, and C-9; H_3-14 → C-3, C-4, and C-5; H_3-15 → C-8, C-9, C-10, and C-7; HRESIMS obsd m/z $[M + Na]^+$ 569.1429, calcd for $C_{30}H_{26}O_{10}Na$, 569.1424.

*Phomalevone C (**3**):* yellow solid; $[\alpha]_D$ +258 (c 4 × 10^{-3} g/mL, $CHCl_3$, 25 °C); UV λ_{max} MeOH (log ε) 209 nm (4.59), 230 (sh, 4.54), 290 (4.15), 379 nm (4.20); ECD (MeOH; $\Delta\varepsilon$) 213 (−106), 235 (+38), 298 (+7), 380 (+3); ^{1}H NMR (400 MHz, $CDCl_3$) δ 13.57 (br s, 8-O*H*), 13.10/13.06 (both br s; 8′-O*H*), 11.82/11.75 (both s, 1-O*H*), 11.51 (br s; 1′-O*H*), 7.01/7.00 (both d, J = 10; H-7′), 6.66/6.65 (both d, J = 0.5; H-4′), 6.614/6.610 (both dd, J = 5.8, 10; H-6), 6.473/6.470 (both d, J = 10; H-6′), 6.421/6.419 (both br s, H-4), 6.223/6.220 (both d, J = 10; H-7), 4.211/4.214 (both br d; 5.8; H-5), 2.089/2.084 (both s; H_3-11′), 2.06/2.01 (both s; H_3-11), 1.68/1.66 (both s; H_3-12′), 1.515/1.511 (both s; H_3-12); ^{13}C NMR (100 MHz, $CDCl_3$) δ 196.2/196.0 (C-5′), 186.79/186.76 (C-9), 185.98/185.97 (C-9′), 162.0/161.9 (C-8′), 159.7/159.6 (C-1′), 159.6/159.5 (C-1), 157.09/157.07 (C-4a), 156.95/156.94 (C-4a′), 151.4/151.3 (C-3′), 150.1/149.8 (C-3), 139.02/138.95 (C-7′), 132.48/132.42 (C-6′), 138.02/137.97 (C-6), 126.7/126.7 (C-7), 117.25/117.20 (C-2′), 116.51/116.46 (C-2), 116.48/116.45 (C-8), 111.3/111.2 (C-8a′), 110.65/110.62 (C-4′), 110.0/109.8 (C-4), 105.4/105.3 (C-9a′), 104.93/104.91 (C-9a), 103.64/103.62 (C-8a), 68.6/68.6 (C-5), 27.0/26.9 (C-12′), 24.0/24.0 (C-12), 21.3/21.3 (C-11′), 21.1, 21.0 (C-11); HMBC correlations ($CDCl_3$, H-# → C-#; includes some four-bond correlations, all of which were relatively weak) 1-O*H* → C-1, C-2, C-3, and C-9a; 1′-O*H* → C-1′, C-2′, C-3′, C-9′, and C-9a′; H-4 → C-2, C-11, C-4a, C-9a, and C-9; H-4′ → C-2′, C-11′, C-4a′, C-9′, and C-9a′; H-6 → C-5, C-8, and C-10a; H-6′ → C-8′ and C-10a′; H-7 → C-5, C-8a, and C-9; H-7′ → C-5′, C-6′, C-8′, C-8a′, and C-9′; H-5 → C-6, C-7, C-8a, C-10a, C-9, and C-12; H_3-11 → C-3 and C-4; H_3-11′ → C-3′ and C-4′; H_3-12 → C-5, C-8a, and C-10a; H_3-12′ → C-5′, C-8a′, and C-10a′; HRESIMS obsd m/z 567.1246 $[M + Na]^+$, calcd for $C_{30}H_{24}O_{10}Na$, 567.1267.

*(R)- and (S)-MPA Esters of Phomalevone A (**1**).* A solution of **1** (1.2 mg) in distilled CH_2Cl_2 (500 μL) was treated with (*S*)-(+)-α-methoxyphenylacetic acid [(*S*)-MPAOH, 2.0 mg, μmoL], DMAP (one crystal), and 1-ethyl-3-(3-dimethylaminopropyl)carbodiimide (1.5 mg, μmoL). The mixture was stirred at 25 °C for 50 h. A 1-mL amount of H_2O was added, and the mixture was extracted with CH_2Cl_2 (3 × 1.5 mL). The combined organic extracts were concentrated, filtered, and evaporated to give a white solid, which was then subjected to HPLC (30 to 100% CH_3CN in H_2O over 45 min) to afford (*S*)-MPA ester **1a** (0.5 mg). Analogous treatment of **1** (1.2 mg) using (*R*)-MPAOH afforded (*R*)-MPA ester **1b** (0.3 mg).

*(S)-MPA ester **1a**:* yellow solid; ^{1}H NMR (400 MHz, $CDCl_3$) δ 13.61 (s, 8-O*H*/8′-O*H*), 11.68 (s, 1-O*H*/1′-O*H*), 6.51 (dd, J = 6.0, 10 Hz, H-6/H-6′), 6.32 (d, J = 10 Hz, H-7/H-7′), 5.82 (d, J = 0.5 Hz, H-4/H-4′), 5.48 (d, J = 6.0 Hz, H-5/H-5′), 1.92 (s, H_3-11/H_3-11′), 1.46 (s, H_3-12/H_3-12′), 7.06−7.29 (5H, m, phenyl group), 4.77 (s, CH), 3.39 (s, OCH_3).

*(R)-MPA ester **1b**:* yellow solid; ^{1}H NMR (400 MHz, $CDCl_3$) δ 13.56 (s, 8-O*H*/8′-O*H*), 11.79 (s, 1-O*H*/1′-O*H*), 6.36 (dd, J = 6.0, 10 Hz, H-6/H-6′), 6.19 (d, J = 10 Hz, H-7/H-7′), 6.20 (d, J = 0.5 Hz, H-4/H-4′), 5.50 (d, J = 6.0 Hz, H-5/H-5′), 2.02 (s, H_3-11/H_3-11′), 1.55 (s, H_3-12/H_3-12′), 7.25−7.37 (5H, m, phenyl group), 4.77 (s, CH), 3.39 (s, OCH_3).

Energy Minimization and ECD Calculations. Conformers of both phomalevone A (**1**) and phomalevone B (**2**) were generated using a constrained dihedral scan. The dihedral angle was constrained between the two inner rings, and geometry optimization was performed every 10 degrees. The resulting minima were optimized again with no constraints, as were their mirror image conformers. All geometry optimizations were performed in the gas phase, and energies of the resulting structures were calculated in the gas phase and in MeOH solution (COSMO solvation model)[35] using resolution-of-identity (RI) approximation and the BP functional,[36,37] combined with the SV(P) basis set[38] and the corresponding auxiliary basis set.[39,40] No symmetry constraints were used during the optimization.

Electronic circular dichroism spectra were calculated for geometries obtained from the RI-BP/SV(P) calculations. Time-dependent density functional calculations (TDDFT) were used with the B3LYP functional[41,42] using the RIJCOSX approximation[43] and TZVP basis set[38] with the corresponding auxiliary basis set.[39,40] A total of 80 excited states were calculated, and only singlet excited states were considered. All of the quantum chemical calculations were performed with ORCA version 2.8.[44] ECD spectra were obtained using SpecDis version 1.50 software.[45] A broadening factor of 0.33 was used in an effort to match the resolution level of the experimental data as closely as possible.

■ ASSOCIATED CONTENT

Supporting Information. ^{1}H and ^{13}C NMR spectra for **1**−**3**. This material is available free of charge via the Internet at http://pubs.acs.org.

■ AUTHOR INFORMATION

Corresponding Author

*Tel: 319-335-1361. Fax: 319-335-1270. E-mail: james-gloer@uiowa.edu.

■ ACKNOWLEDGMENT

We thank the staff of the University of Iowa High-Field NMR and Mass Spectrometry Facilities and Mr. S. Neff and Mr. N. Phatak for technical assistance. Support for this work from the National Science Foundation (CHE-0718315 to J.B.G. and AGS 0927944 to J.B.) is gratefully acknowledged, and a postdoctoral fellowship (to S.H.S.) from the Korea Research Foundation (E00075) is also appreciated. USDA is an equal opportunity provider and employer.

■ DEDICATION

Dedicated to Professor Koji Nakanishi of Columbia University in honor of his pioneering work on bioactive natural products.

■ REFERENCES

(1) Schmidt, L. E.; Deyrup, S. T.; Baltrusaitis, J.; Swenson, D. C.; Wicklow, D. T.; Gloer, J. B. *J. Nat. Prod.* **2010**, *73*, 404–408.

(2) Gloer, J. B. In *The Mycota*, 2nd ed.; Kubicek, C. P.; Druzhinina, I. S., Eds.; Springer-Verlag: New York, 2007; Vol. IV, pp 257−283.
(3) Sy, A. A.; Swenson, D. C.; Gloer, J. B.; Wicklow, D. T. *J. Nat. Prod.* **2008**, *71*, 415–419.
(4) Shim, S. H.; Swenson, D. C.; Gloer, J. B.; Dowd, P. F.; Wicklow, D. T. *Org. Lett.* **2006**, *8*, 1225–1228.
(5) Wicklow, D. T.; Joshi, B. K.; Gamble, W. R.; Gloer, J. B.; Dowd, P. F. *Appl. Environ. Microbiol.* **1998**, *64*, 4482–4484.
(6) Isaka, M.; Jaturapat, A.; Rukseree, K.; Danwisetkanjana, K.; Tanticharoen, M.; Thebtaranonth, Y. *J. Nat. Prod.* **2001**, *64*, 1015–1018.
(7) Isaka, M.; Palasarn, S.; Kocharin, K.; Saenboonrueng, J. *J. Nat. Prod.* **2005**, *68*, 945–946.
(8) Steyn, P. *Tetrahedron* **1970**, *26*, 51–57.
(9) Ohtani, I.; Kusumi, T.; Kashman, Y.; Kakisawa, H. *J. Am. Chem. Soc.* **1991**, *113*, 4092–4096.
(10) Latypov, S. K.; Seco, J. M.; Quinoa, E.; Riguera, R. *J. Org. Chem.* **1996**, *61*, 8569–8577.
(11) Fujimoto, H.; Asai, T.; Kim, Y.; Ishibashi, M. *Chem. Pharm. Bull.* **2006**, *54*, 550–553.
(12) Frank, B.; Flasch, H. *Prog. Chem. Org. Nat. Prod.* **1973**, *30*, 151.
(13) Andersen, R.; Buchi, G.; Kobbe, B.; Demain, A. *J. Org. Chem.* **1977**, *42*, 352–353.
(14) Kawahara, N.; Sekita, S.; Satake, M.; Udagawa, S.; Kawai, K. *Chem. Pharm. Bull.* **1994**, *42*, 1720–1723.
(15) He, H.; Bigelis, R.; Solum, E. H.; Greenstein, M.; Carter, G. T. *J. Antibiot.* **2003**, *56*, 923–930.
(16) Jaroszewski, J.; Storm-Hansen, T.; Hansen, L. *Chirality* **1992**, *4*, 216–221.
(17) Bringmann, G.; Hinrichs, J.; Henschel, P.; Kraus, J.; Peters, K.; Peters, E.-M. *Eur. J. Org. Chem.* **2002**, 1096–1106.
(18) Sakurai, N.; Akatsuka, H.; Minakami, J.; Nishio, M.; Kono, O.. *Jpn. Kokai Tokkyo Koho* JP 2004075625, 2004.
(19) Chutrakul, C.; Boonruangprapa1, T.; Suvannakad1, R.; Isaka1, M.; Sirithunya, P.; Toojinda, T.; Kirtikara, K. *J. Appl. Microbiol.* **2009**, *107*, 1624–1631.
(20) Ondeyka, J. G.; Dombrowski, A. W.; Polishook, J. P.; Felcetto, T.; Shoop, W. L.; Guan, Z.; Singh, S. B. *J. Antibiot.* **2006**, *59*, 288–292.
(21) Yoganathan, K.; Cao, S.; Crasta, S. C.; Aitipamula, S.; Whitton, S. R.; Ng, S.; Buss, A. D.; Butler, M. S. *Tetrahedron* **2008**, *64*, 10181–10187.
(22) Wagenaar, M. M.; Clardy, J. *J. Nat. Prod.* **2001**, *64*, 1006–1009.
(23) Stewart, M.; Capon, R. J.; White, J. M.; Lacey, E.; Tennant, S.; Gill, J. H.; Shaddock, M. P. *J. Nat. Prod.* **2004**, *67*, 728–730.
(24) Kachi, H.; Sassa, T. *Agric. Biol. Chem.* **1986**, *50*, 1669–1671.
(25) Schmidt, W.; Beerhues, L. *FEBS Lett.* **1997**, *420*, 143–146.
(26) Hill, J. G.; Nakashima, T. T.; Vederas, J. C. *J. Am. Chem. Soc.* **1982**, *104*, 1745–1748.
(27) Bauer, A. W.; Kirby, W. M.; Sherris, J. C.; Turck, M. *Am. J. Clin. Pathol.* **1966**, *45*, 493–496.
(28) Wagenaar, M. M.; Clardy, J. *J. Nat. Prod.* **2001**, *64*, 1006–1009.
(29) Jiao, P.; Swenson, D. C.; Gloer, J. B.; Campbell, J.; Shearer, C. A. *J. Nat. Prod.* **2006**, *69*, 1667–1671.
(30) Höller, U.; Gloer, J. B.; Wicklow, D. T. *J. Nat. Prod.* **2002**, *65*, 876–882.
(31) Boerema, G. H.; de Gruyter, J.; Noordeloos, M. E.; Hamers, M. E. C. *Phoma Identification Manual. Differentiation of Specific and Infraspecific Taxa in Culture*; CABI Publishing: Wallingford, UK. 2004.
(32) de Gruyter, J.; Woudenberg, J. H. C.; Aveskamp, M. M.; Verkley, G. J. M.; Groenewald, J. Z.; Crous, P. W. *Mycologia* **2010**, *102*, 1066–1081.
(33) O'Donnell, K. *Sydowia* **1996**, *48*, 57–70.
(34) White, T. J.; Bruns, T.; Lee, S.; Taylor, J. W. In *PCR Protocols: a Guide to Methods and Applications*; Innis, M. A., Gelfand, D. H., Sninsky, J. J., White, T. J., Eds.; Academic Press: New York, 1990; pp 315−322.
(35) Sinnecker, S.; Rajendran, A.; Klamt, A.; Diedenhofen, M.; Neese, F. *J. Phys. Chem. A* **2006**, *110*, 2235–2245.
(36) Perdew, J. P. *Phys. Rev. B* **1986**, *33*, 8822–8824.
(37) Becke, A. D. *Phys. Rev. A* **1988**, *38*, 3098–3100.
(38) Schaefer, A.; Horn, H.; Ahlrichs, R. *J. Chem. Phys.* **1992**, *97*, 2571–2577.
(39) Eichkorn, K.; Weigend, F.; Treutler, O.; Ahlrichs, R. *Theor. Chim. Acta* **1997**, *97*, 119–124.
(40) Eichkorn, K.; Treutler, O.; Öhm, H.; Häser, M.; Ahlrichs, R. *Chem. Phys. Lett.* **1995**, *240*, 283–289.
(41) Becke, A. D. *J. Chem. Phys.* **1993**, *98*, 5648–5652.
(42) Lee, C.; Yang, W.; Parr, R. G. *Phys. Rev. B* **1988**, *37*, 785–789.
(43) Neese, F.; Wennmohs, F.; Hansen, A.; Becker, U. *Chem. Phys.* **2009**, *356*, 98–109.
(44) Neese, F. *ORCA*, Version 2.8.0; Universität Bonn: Bonn, Germany, 2010.
(45) Bruhn, T.; Hemberger, Y.; Schaumlöffel, A.; Bringmann, G. *SpecDis*, Version 1.50; Universität Würzburg: Würzburg, Germany, 2010.